MECHANIKA TEORETYCZNA
I STOSOWANA
Journal of Theoretical
and Applied Mechanics
4, 30, 1992

TWO–DIMENSIONAL APPROACH TO THE ANALYSIS OF PHASE TRANSFORMATION KINETICS IN STEEL HARDENING PROCESSES

JERZY WOELKE

JERZY ZIELNICA

Technical University of Poznań

The paper presents a method for determination of a phase transformation kinetics in cylindrial steel bodies with an arbitrary shaped cross–section. The analysis is presented for a two–dimensional region, where the heat flow on the edges of the region appears. The solution of the problem is based on variational–difference method, being a combination of the finite element method and the finite difference method. The results are the basis for evaluation of temporary and residual stress distribution in self–cooling processes.

1. Introduction

The aim of this work is to develop a numerical method for the analysis of the kinetics of phase transformations in the hardening process of cylindrical bodies of any cross–section made of carbon steel.

The object of calculations refers only to steel grades displaying C–shaped $T-T-T$ curves with a carbon content close to that of eutectoidal steel. The computations were madefor different cooling rates (characterized by the dimensionless Biot number Bi) as well as for different time intervals to achieve halfthe full austenite into pearlite trensformation $\tau_{0.5}$.

The obtained results will be used in our further works for the estimation of the distribution of transient and residualstresses appearing in the process of hardening.

We assume that the heat exchange in such a body occurs on the boundary of one of the two dimensions of the field (thereby the discussed problem becomes independent of variable z).

The determined field of temperature $T(x, y, t, \mathrm{Bi})$ will be the basis for the kinetics of phase transformations analysis.

The authors (cf [1,9]) dealing with one–dimensional problems reported that they have succeeded in obtaining an analytical solution in the form of an infinite

series. In the analysis of the temperature field varying in time for an optional planar field with the boundary conditions of another type (as it is in our work), it is not possible to obtain an analytical solution. Therefore, we apply here the variational–finite difference method being a combination of the Finite Difference Method (FDM) and a variational method [10].

The solutions are based on the experimental data of Lomakin (cf [2,3,4]) and on the theory of Inoue and Raniecki [5], as well as on the model of Ericson and Hildenwall [6]. An algorithm has been presented, being the basis for the computer simulation of hardening stresses generation process.

The stresses propagation in the hardening process occurs due to the non–uniform thermal expansion and the non–free change of the specific volume of the particular structures and phases.

The (relative) volume of the element during the transformation of austenite into martensite, depending on the chemical composition of a steel and a number of other factors, can be changedwithin the limits of several percent. During the transformation of austenite into pearlite the element is subject to a slightly smaller volume change, but this change is also comparable with the decrease of volume due to the thermal contraction caused the difference of temperature equal to 1000 K. We have determined in our work the weight fraction of austenite, pearlite and martensite, and we have accepted the thermomechanical properties of bainite as being equal to those of pearlite. With the fixed distribution of temperature fields and the weight (volume) fractions of austenite, pearlite and martensite we have calculated the relative change of volume ε^T of the material assuming that the phase transformations occur within the elastic range.

2. Basic analytical equations of heat transfer with phase transformations

The problem of heat transfer consists in finding a temperature field satisfying the differential equation together with the accompanying boundary conditions and the initial condition. As a result of this solution, we obtain a function of temperature in the coordinates x, y, of the investigated point, time t, and the dimensionless Biot number Bi, respectively.

$$T = T(x, y, t, \mathrm{Bi}) \tag{2.1}$$

$$\mathrm{Bi} = \frac{\alpha}{\lambda} l$$

where α is the heat transfer coefficient on the body surface, λ is the coefficient of thermal conductivity, l is the characteristic dimension. This solution depends

in parametrical way on the Biot number, representing the cooling rate and on material properties that also depend on Biot number. This dependence expressed by a non-linear equation and its solution generally requires the application of numerical methods. Among the existing numerical methods we have chosen the finite elements method. The investigated field was divided intoan adequate number of elements and nodes and the function of temperature fields inside the elements depending on the temperature of nodes was assumed.

The general form of the solution is the following one

$$T = \sum_i H_i T_i \tag{2.2}$$

where: H is the shape functions, T_i is the temperature at the ith node.

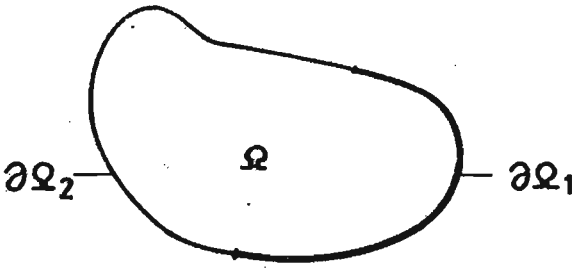

Fig. 1. Region Ω

Having in mind the application of the Finite Element Method to the determination of temperature field in the planar areas let us analyse the equation of heat transfer over the area Ω (Fig.1) in the form

$$\frac{\partial}{\partial x}\left(\lambda\frac{\partial T}{\partial x}\right) + \frac{\partial}{\partial y}\left(\lambda\frac{\partial T}{\partial y}\right) = c\rho\frac{\partial T}{\partial t} \tag{2.3}$$

with the initial condition

$$T(x,y,t)\Big|_{t=0} = T_0(x,y) \tag{2.4}$$

and with the following boundary conditions

$$\begin{aligned} -\lambda\frac{\partial T}{\partial n} &= \alpha(T - T_0) && \text{at the boundary } \partial\Omega_1 \\ \lambda\frac{\partial T}{\partial n} &= 0 && \text{at the boundary } \partial\Omega_2 \end{aligned} \tag{2.5}$$

where: T_0 is the initial temperature at the boundary $\partial\Omega_1$, c is the specific heat, ρ is the density.

We assume that Eq (2.3) with conditions (2.4) and (2.5) has an exactly one solution. For the solution to Eq (2.3) we apply the variational–finite difference method being a combination of the Finite Element Method and the variational method. The first method is applied with respect to variables x, y, and the second one to the time variable t.

In order to reduce Eq (2.3) to the variational one, we apply the Galerkin's procedure.

For this purpose we multiply Eq (2.3) by a function $v \in R^1$, and then we integrate it over the area Ω.

$$\iint_{\Omega} \Big[\frac{\partial}{\partial x}\Big(\lambda\frac{\partial T}{\partial x}\Big) + \frac{\partial}{\partial y}\Big(\lambda\frac{\partial T}{\partial y}\Big)\Big] v dx dy = \iint_{\Omega} c\rho\frac{\partial T}{\partial t} v dx dy \tag{2.6}$$

rApplying boundary conditions (2.4) and (2.5) we obtain

$$\begin{aligned} &\iint_{\Omega}\Big(\lambda\frac{\partial T}{\partial x}\frac{\partial v}{\partial x} + \lambda\frac{\partial T}{\partial y}\frac{\partial v}{\partial y}\Big) v dx dy + \\ &+ \iint_{\Omega} c\rho\frac{\partial T}{\partial t} v dx dy - \int_{\partial\Omega_1} \alpha(T - T_0) v ds = 0 \end{aligned} \tag{2.7}$$

Therefore, the solution of the problem (2.3) is reduced to the solution (2.7). We look for the solution $T(x, y, t)$ in the form

$$T(x, y, t) = \sum_{l=1}^{W} T_l(t) H_l(x, y) \tag{2.8}$$

The functions $H_l(x, y)$ are the shape functions and they are the base of finite–dimensional space V_m. They are explicitly defined by the functions of coordinates. They have to be continuous functions (also when passing from one element to another) and their first derivative has to be defined and different from zero. Let us note the important property of these functions within the element.

From Eq (2.8) it follows that

$H_i = 1$ for the i–th node

$H_i = 0$ for the remaining nodes.

As soon as we define the shape of the element and its corresponding function, the further operations will be carried out according to the standard scheme. By substituting the solution (2.8) into (2.7) and substituting for $v = H_k$ we obtain

$$\sum_{l=1}^{W} T_l(t) \iint_{\Omega} \lambda\Big(\frac{\partial H_l}{\partial x}\frac{\partial H_k}{\partial x} + \frac{\partial H_l}{\partial y}\frac{\partial H_k}{\partial y}\Big) dx dy +$$

$$+\sum_{l=1}^{W}\frac{\partial T_l(t)}{\partial t}\iint_{\Omega} c\rho H_l H_k dx dy - \tag{2.9}$$
$$-\sum_{l=1}^{W} T_l(t)\int_{\partial\Omega_1}\alpha H_l H_k ds + \int_{\partial\Omega_1}\alpha T_0 H_k ds = 0$$

with the initial condition

$$\sum_{l=1}^{W} T_l(0)H_l(x,y) = T_0(x,y) \tag{2.10}$$

Taking in Eq (2.9) for $k = 1,2,3,...$ we obtain a system of differential equations

$$\mathbf{C}\frac{dT(t)}{dt} + \mathbf{A}T(t) = \mathbf{B}$$
$$T(x,y,t)\Big|_{t=0} = T_0(x,y) \tag{2.11}$$

This system is solved by the application of differential approximation over time. For this purpose we construct a mesh ω_t for $[0,T]$ in the form

$$\omega_t = \left\{t: \quad t = n\Delta t; \quad n = 0,1,...,H, \quad H\Delta t = T\right\} \tag{2.12}$$

Accepting the following

$$T_l(n\Delta t) = T_l^n \tag{2.13}$$

the problem (2.11) is approximated by the following finite difference scheme

$$\mathbf{C}\frac{T^{n+1} - T^n}{\Delta t} + \mathbf{A}\frac{T^{n+1} + T^n}{2} = \mathbf{B} \tag{2.14}$$

(where: T_0 is fixed by the initial condition).

It is so called Crank–Nicolson scheme [10].

To the diagonal elements A_{ii} of the principal matrix $\mathbf{A}$, we add the term $2c\rho V_i(\Delta t)$, while the vector of constans elements B_i^k are increased by the terms

$$B_i^{k-1} + \sum_j A_{ij}T_j^{k-1} \tag{2.15}$$

where the summing up takes place throughout all non–zero elements of the ith row.

If the thermophysical properties depend on the temperature, we determine them for the temperature corresponding to the half of the time step.

Following the procedural scheme according to the Crank–Nicolson method leads us to the equation system in temperatures T_i^k solved at each time step.

In the first step, after the differential division and the numbering of nodes, we determine the indices of neighbouring points and boundary nodes. Then, we conctruct the matrix of the system modifying only the entries of the principal diagonal, and in the further part we construct the vector of constants.

In order to determine from Eq (2.11) the matrices **A**, **B**, **C**, occurring in Eq (2.14), we must determine the integral expression over the area Ω (first and second Eq (2.9)).

For the caculation of these integrals we transform the real elements of coordinates x, y, into unity elements with coordinates ξ, η, and we use the standard FEM procedure described by Irons and Ahmad [10]. The integrals are calculated numerically using the Gauss–Legendre metod.

Let us analyse now the curvilinear integral over the boundary $\partial\Omega_1$ (see Eq (2.9))

$$\int_{\partial\Omega_1} \alpha H_l H_k ds \qquad \text{and} \qquad \int_{\partial\Omega_1} \alpha T_0 H_k ds \tag{2.16}$$

We assume that the boundary $\partial\Omega_1$ is a regular curve, i.e. it can be divided into a finite number of smooth arcs.

This division follows from the discretization of the $2D$ continuum into the quadrilateral elements. The boundary $\partial\Omega_1$ is defined by the subset i^B of the successive boundary nodes.

$$i^B = \left\{ i_1^B, i_2^B, ..., i_{WB}^B \right\} \tag{2.17}$$

where: WB – indicates the number of boundary nodes.

Calculationg curvilinear integrals from Eq (2.16) we use the formulas

$$\int_{\partial\Omega_1} \alpha H_l H_k ds = \int_{i_1^B i_2^B} \alpha H_l H_k ds + \int_{i_2^B i_3^B} \alpha H_l H_k ds + ... + \int_{i_{WB-1}^B i_{WB}^B} \alpha H_l H_k ds \tag{2.18}$$

$$\int_{\partial\Omega_1} \alpha T_0 H_k ds = \int_{i_1^B i_2^B} \alpha T_0 H_k ds + ... + \int_{i_{WB-1}^B i_{WB}^B} \alpha H_l H_k ds \tag{2.19}$$

For the calculation of the curvilinear integral of the form

$$\int_s f(x,y) ds \tag{2.20}$$

the regular arc s is presented in the parametrical form

$$x = x(r) \qquad y = y(r) \qquad -1 \le r \le +1 \tag{2.21}$$

Then

$$\int_s f(x,y)ds = \int_{-1}^{+1} f\Big(x(r),y(r)\Big)\sqrt{x_{,r}^2 + y_{,r}^2}\,dr \tag{2.22}$$

Let us analyse the segment of the boundary between the successive boundary nodes $W1$ and $W2$, Fig.2.

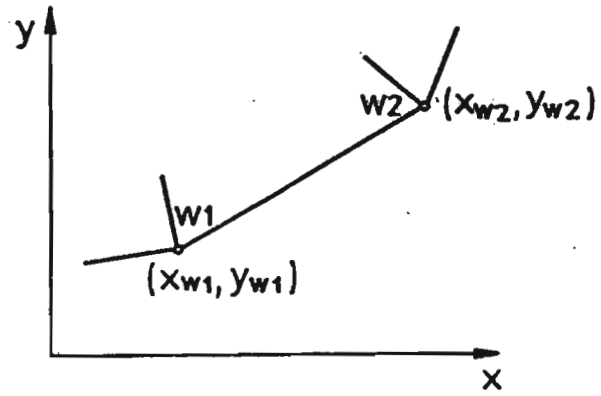

Fig. 2. Element boundary section

This section is parametrically represented

$$\begin{aligned} x(r) &= \frac{x_{W2} - x_{W1}}{2}r + \frac{x_{W2} + x_{W1}}{2} \\ y(r) &= \frac{y_{W2} - y_{W1}}{2}r + \frac{y_{W2} + y_{W1}}{2} \end{aligned} \tag{2.23}$$

In this case

$$\int_s f(x,y)ds = \frac{1}{2}\int_{-1}^{+1} f\Big(x(r),y(r)\Big)G(x,y)dr \tag{2.24}$$

where

$$G(x,y) = \sqrt{(x_{W2} - x_{W1})^2 + (y_{W2} - y_{W1})^2} \tag{2.25}$$

A_{kl} will be different from zero in the following three cases

(a) $k = W1$ $l = W1$
(b) $k = W1$ $l = W2$ or vice versa
(c) $k = W2$ $l = W2$

$$A_{kl} = \int_{W1}^{W2} \alpha H_k H_l ds \tag{2.26}$$

Thus we have

$$(a) \qquad A_{kl} = \frac{1}{4}G(x,y)\int_{-1}^{+1}\alpha(1-r)(1-r)dr$$

$$(b) \qquad A_{kl} = \frac{1}{4}G(x,y)\int_{-1}^{+1}\alpha(1-r)(1+r)dr \tag{2.27}$$

$$(c) \qquad A_{kl} = \frac{1}{4}G(x,y)\int_{-1}^{+1}\alpha(1+r)(1+r)dr$$

We proceed in an analogical way calculating

$$B_k = \int_{W1}^{W2}\alpha H_k T_0 ds \tag{2.28}$$

This integral on segment $W1, W2$ is different than zero only for

$$k = W1 \qquad \text{and} \qquad k = W2$$

In these cases

$$B_{W1} = \frac{1}{4}G(x,y)\int_{-1}^{+1}\alpha(1-r)T_0 dr$$

$$B_{W2} = \frac{1}{4}G(x,y)\int_{-1}^{+1}\alpha(1+r)T_0 dr \tag{2.29}$$

For the calculation of integrals (2.35) and (2.38) we use the Gauss–Legendre method of numerical integration. In this way, integrating along the boundary and over the elements, we determine the system of equation coefficients

$$\mathbf{A}\left[T^{n+1}\right] = \mathbf{B} \tag{2.30}$$

The solution to Eqs (2.30) results in the required temperature field $\left[T^{n+1}\right]$ for $t = (n+1)\Delta t$ in all nodal points of the analysed 2–dimensional area Ω.

3. Basic equations of phase transformation kinetics

After determination of the transient temperature fields, we proceed to the calculation of the weight fractions of pearlite p_1 and martensite m_1, and the

relative volumetric change. Below we discuss briefly the basic formulae necessary for the formulation of the algorithm of the simulation of phase transformations acompanying the hardening process.

As we know, the transformation of austenite into pearlite $A \rightarrow P$ has a diffusive character. It belongs to the transformation group of nucleation and growth (cf [7]).

a. In constant temperature $T < T_A$ (T_A is the temperature of the end of austenite transformation) the amount of transformation product p_1 (weight fraction of pearlite[1]) grows in time until the moment when the free energy of the steel element reaches the minimal value.

b. The speed of transformation $\dot{p}_1 = \frac{dp_1}{dt}$ depends in an essential way on the actual value p_1 and the temperature T. Within the temperature range $T < M_s$ the transformation occurs practically of a negligible speed, (M_s is the temperature at which the martensitic transformation begins).

c. The significant preliminary plastic strains and stresses affect the course of the transformation.

d. In rather a wide range of temperatures the nuclei appear mainly on the borders of austenite grains. Therefore, the speed of transformation depends on the grain border size.

In the paper we do not take into consideration the assumptions of c and d given above.

We are going to use the following dimensionless values

$$\Theta = \frac{T}{T_0} \qquad \bar{x} = \frac{x}{l}$$
$$\bar{y} = \frac{y}{l} \qquad \tau = \frac{\kappa t}{l^2} \tag{3.1}$$

where $\kappa = \lambda / c\rho$ is thermal diffusivity.

In order to determine the weight fraction p_1, we assume after Can (cf [8]) and after Inoue and Raniecki [5] the model of isokinetic transformation

$$p_1 = G_1(z) \qquad z(\bar{x}, \bar{y}, \tau) = \int f_1\Big(\Theta(\bar{x}, \bar{y}, \tau)\Big) d\tau \tag{3.2}$$

and

$$f_1(\Theta) = \begin{cases} 0 & \text{for } \Theta_1 > T_A \\ f(\Theta_1)\frac{1}{\tau_{0.5}} & \text{for } \Theta_1 \leq \bar{T}_A \end{cases} \tag{3.3}$$

where

$$\Theta_1(\bar{x}, \bar{y}, \tau) = \frac{\bar{T}_A - \Theta(\bar{x}, \bar{y}, \tau)}{\bar{T}_A - \bar{T}_1} \tag{3.4}$$

$$f(\Theta_1) = \left[1 - \exp(-7\Theta_1^{2.5})\right] \exp\left[-2.6(1-\Theta_1)^2\right] \tag{3.5}$$

In Eq (3.2) both $G_1(z)$ and $f_1(\Theta)$ can be determined from the usual isothermal time–temperature–transformation (T–T–T) diagrams [5].

We can determine the weight fraction at pearlite in each point of the area x = constat and at each instant τ.

From the analysis of the formulae for p_1 it follows that p_1 depends on four dimensionless parameters

$$p_1 = p_1(\mathrm{Bi}, \bar{T}_A, \bar{T}_1, \tau_{0.5}) \tag{3.6}$$

$$\bar{T}_A = \frac{T_A}{T_0} \qquad \bar{T}_1 = \frac{T_1}{T_0} \qquad \tau_{0.5} = \frac{\kappa t_{0.5}}{l^2}$$

where T_A – is the temperature of the beginning of the isothermic transformation of austenite into pearlite. T_1 – is the temperature of the least durability of the isothermic disintegration of austenite into pearlite, $t_{0.5}$ is the time interval of half disintegration of austenite into pearlite at temperature T_1.

The dimensionless parameters $\bar{T}_A$ and $\bar{T}_1$ accepted for different steel grades differ significantly, therefore the calculations are done for the following data of these parametres

$$\bar{T}_A = 0.95 \qquad \bar{T}_1 = 0.75$$

The weight fraction of martensite is calculated from the formula

$$m_1 = (1 - p_1)\bar{m}_1(T) \tag{3.7}$$

where the function $\bar{m}_1(T)$ is determined by the weight fraction of martensite in the case when the transformation $A \to P$ does not occur

$$\bar{m}_1(T) = \begin{cases} 0 & \text{for } T > M_s \\ m_2(T) & \text{for } M_s \geq T \geq T_r \end{cases} \tag{3.8}$$

In the above formulae, M_s is the temperature at which the martensitic transformation begins and T_r is the room temperature. Inove and Raniecki [5] defined the function $m_2(T)$ applying the experimental results obtained by Lomakin [2]

$$m_2(T) = (1 - a_r)\Phi(\Theta_2) \tag{3.9}$$

where

$$\Theta_2 = \frac{M_s - T}{M_s - M_f} \tag{3.10}$$

$$\Phi(\Theta_2) = \left[1 - (1-\Theta_2)^{2.5} H(1-\Theta_2)\right]\left[1 - \exp(-17\Theta_2^2)\right] \tag{3.11}$$

where a_r is the residual austenite, symbol H is the Heaviside function, and M_f is the temperature at which the martensitic transformation ends. The function Θ_2 can be expressed by dimensionless values in the following way

$$\Theta_2(\bar{x},\bar{y},\tau) = \frac{\bar{T}_s - \Theta(\bar{x},\bar{y},\tau)}{\bar{T}_s - \bar{T}_f} \tag{3.12}$$

where

$$\bar{T}_s = \frac{M_s}{T_0} \qquad \bar{T}_f = \frac{M_f}{T_0} \tag{3.13}$$

Hence, it follows that the actual content of martensite depends on seven dimensionless parameters

$$m_1 = m_1(\mathrm{Bi}, \bar{T}_A, \bar{T}_1, \bar{T}_s, \bar{T}_f, \tau_{0.5}, a_r) \tag{3.14}$$

Knowing the temperature distribution and the weight fractions of pearlite and martensite, we determine the relative change of volume

$$\varepsilon^T = p_1(\gamma_1 - \alpha_1 T) + m_1(\gamma_2 - \alpha_2 T) + \alpha_A(T - T_0) \tag{3.15}$$

where α_A is the mean coefficient of the linear thermal expansion of austenite, but α_1 and α_2 differ from the thermal expansion coefficients of pearlite and martensite, respectively; although they directly depend on them. If $\alpha_1 = \alpha_2 = \alpha_A = 0$, then we obtain a simple model neglecting the thermal expansion of all components. The parameters γ_1 and γ_2 are dimensionless constants depending on the carbon content γ, the initial temperature T_0, and the relative volume changes accompanying the transformations of $A \to P$ (austenite into pearlite) and $A \to M$ (austenite into pearlite), respectively

$$\begin{aligned}
&\alpha_1 = \frac{1}{\omega}(1.01 + 0.03\gamma)10^{-3}{}^{\circ}\mathrm{C}^{-1} && \alpha_2 = 1.37\frac{1}{\omega}10^{-3}{}^{\circ}\mathrm{C}^{-1} \\
&\alpha_A = 2.85\frac{1}{\omega}10^{-3}{}^{\circ}\mathrm{C}^{-1} && \gamma_1 = \frac{1}{\omega}(1.42 - 0.56\gamma) \\
&\gamma_2 = \frac{1}{\omega}(1.42 + 0.21\gamma) && \omega = 122.82 + 2.15\gamma + 8.56 \cdot 10^{-3}T_0
\end{aligned} \tag{3.16}$$

where T_0 should be expressed in $^{\circ}\mathrm{C}$, and γ is the percentage (Wt) content of C (cf [5]).

Eq (3.15) in dimensionless quantities

$$\bar{\varepsilon}^T = \frac{\varepsilon^T}{\alpha_A T_0} \qquad \bar{\gamma}_1 = \frac{\gamma_1}{\alpha_A T_0} \qquad \bar{\gamma}_2 = \frac{\gamma_2}{\alpha_A T_0}$$

$$\bar{\alpha}_1 = \frac{\alpha_1}{\alpha_A} \qquad \bar{\alpha}_2 = \frac{\alpha_2}{\alpha_A}$$

depends on eleven parameters

$$\bar{\varepsilon}^T = \bar{\varepsilon}^T(\mathrm{Bi}, \bar{T}_A, \bar{T}_1, \tau_{0.5}, \bar{T}_s, \bar{T}_f, a_\tau, \bar{\gamma}_1, \bar{\gamma}_2, \bar{\alpha}_1, \bar{\alpha}_2) \tag{3.17}$$

In the calculations, for steel with 0.8% carbon content, the following experimental results of Lomakin have been accepted

$$\begin{aligned} \bar{\gamma}_1 &= 0.44 \qquad & \bar{\gamma}_2 &= 0.71 \\ \bar{\alpha}_1 &= 0.36 \qquad & \bar{\alpha}_2 &= 0.48 \end{aligned} \tag{3.18}$$

4. Discussion of the numerical calculations algoritm and a numerical example

The program of numerical calculations is written in FORTRAN 77. This program consists of two parts. The first part calculates the temperature field varying in time $\Theta(x, y, t)$ for an optional 2–dimensional material area, which can be devided into finite elements.

The second part of the program refers to the analysis of the kinetics of phase transformations and basing on thetemperature field $\Theta(\bar{x}, \bar{y}, \tau)$ determined in the first part, it calculates the weight fractions of pearlite p_1 and martensite m_1, respectively, together with the relative change of volume ε^T.

The program is constructed in such a way that after the data collection, there follows the linking of nodes and elements, and a control printout of the basic values like:physical and geometric parameters, mesh of finite elements, characteristic temperatures. The field of temperatures $\Theta(x, y, \tau)$ determined in the first part of the program is stored in the memory for the second part to be used in.

Additionally, in order to speed up the calculations when some parameters are changed, the field of temperatures is stored in a binary file.

For the integration of some functions occurring in the connections of the kinetics of phase transformations, the numerical methods are applied (Romberg's method and the trapezoid method).

Two forms of the printout have been provided for the interesting values: the full printout (the field of temperatures and p_1, m_1, $\bar{\varepsilon}^T$), and also an abbreviated printout (only the values referring to the kinetics of phase transformations). The relative change of volume was calculated both according to Lomakin's theory [2,3,4] and according to the modification by Inoue–Raniecki [5].

The purpose of the numerical calculations is the presentation of the developed part of the computer system referring to the two–dimensional problems and

to the investigation of the influence of the basic physical and geometric parameters of the considered object on the temperature field and the kinetics of phase transformations.

A spline shaft has been selected ($n = 8$) of 0.22 m in diameter (n is the number of splines). We have assumed that the length of the rod was large in comparison with the dimensions of the cross–section and that heat was carried away uniformly along the whole perimetr of the cross–section.

Fig.3 presents a scheme together with the dimensions of thediscussed cross–section and the division into finite elements.

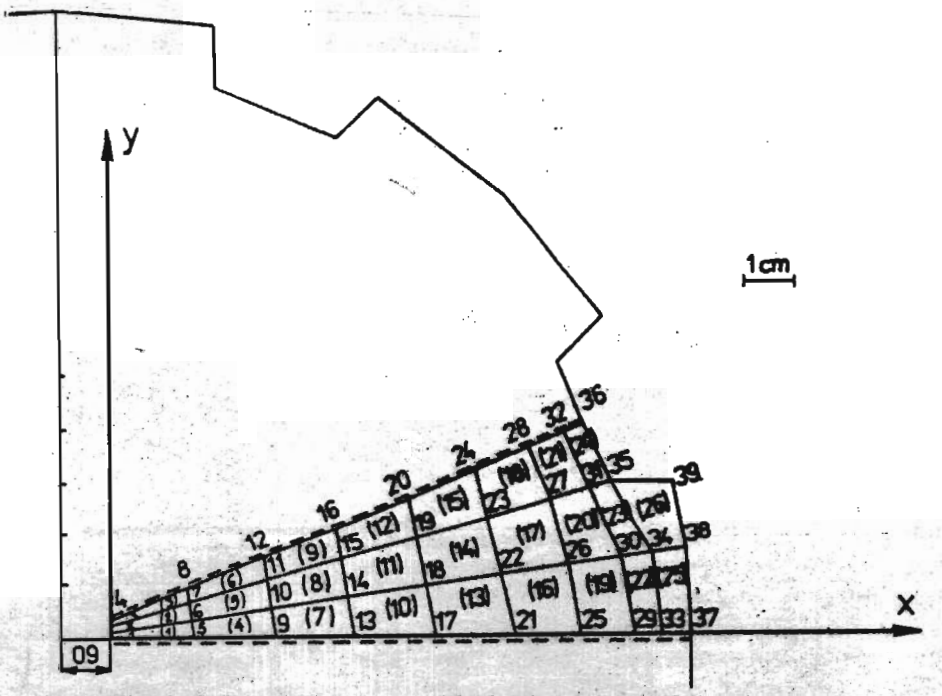

Fig. 3. Spline shaft scheme with the division into finite elements

The analysis of the spline shaft was carried out for the perimeter of the cross–section. The analysis of the spline shaft cross–section was carried out for 1/16th of the whole cross–section area, utilizing the repeatability of the shape and the course of the heat exchange for the particular sectors. An isolation (no heat exchange) was assumed here along all boundary elements, with the exception of 36-35, 35-39, 39-38, 38-37 – since these elements, referred to the free boundary contacting with the surrounding. The division was made into 26 non–normalized finite elements with 39 nodes. The same material parameters have been accepted here as in the previous work [9], but the characteristic dimension was $l = 0.11$ m.

We have assumed that the analysed spline shaft was uniformly heated to the temperature of 1053° K, and then suddenly immersed in a cooling medium. The following basic parameters have been assumed

$$\lambda = 40\frac{\mathrm{W}}{\mathrm{m\,K}} \qquad c = 800\frac{\mathrm{J}}{\mathrm{kg\,K}} \qquad \rho = 7800\frac{\mathrm{kg}}{\mathrm{m}^3}$$

$$\alpha = 13300\frac{\mathrm{W}}{\mathrm{m}^2\mathrm{K}} \qquad \tau_{0.5} = 0.1$$

Basing on prepared sets of data, a program of numerical calculations was excented and basing on the obtained results a series of plots were prepared.

Fig.4 illustrates the temperature distribution over the cross–section of the spline shaft as the function of time, in selected mesh nodes of the finite elements division.

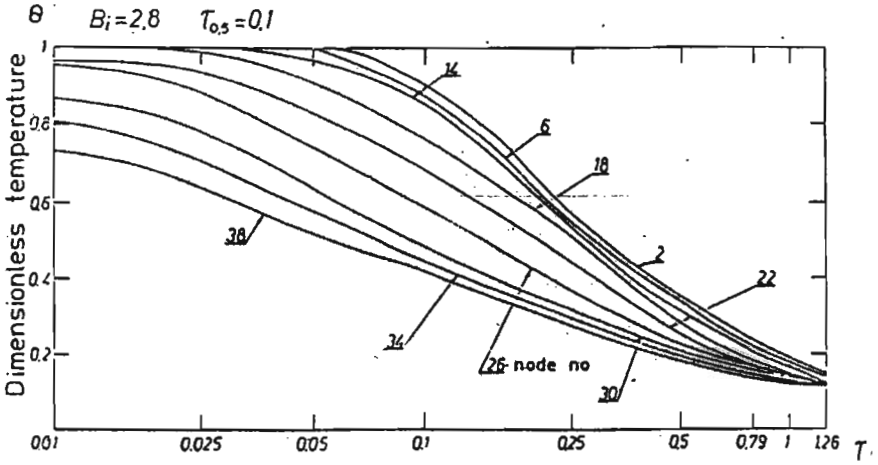

Fig. 4. Temperature distribution in spline shaft cross–section

It follows from this figure that during the starting period of cooling, the temperature suddenly drops, but in the core it is constant for a longer time. Hence, during the first period of time, no transformations take place, the core is compressed and the shaft surface is tensioned.

The dimensionless values $\bar{\varepsilon}^T$ (Fig.6) at the nodes 16,30,34,38, start to decrease. In this period, the thermal deformations practically do not play any role. So, after the hardening process ends, the layers lying close to the surface are compressed what is connected with the transformation of $A \rightarrow M$ (austenite into martensite) since intensionless condition the volume of the element would increase.

The transformations $A \rightarrow P$ (austenite into pearlite) and $A \rightarrow M$ (austenite into martensite), respectively (Fig.5), taking place in the second period of time

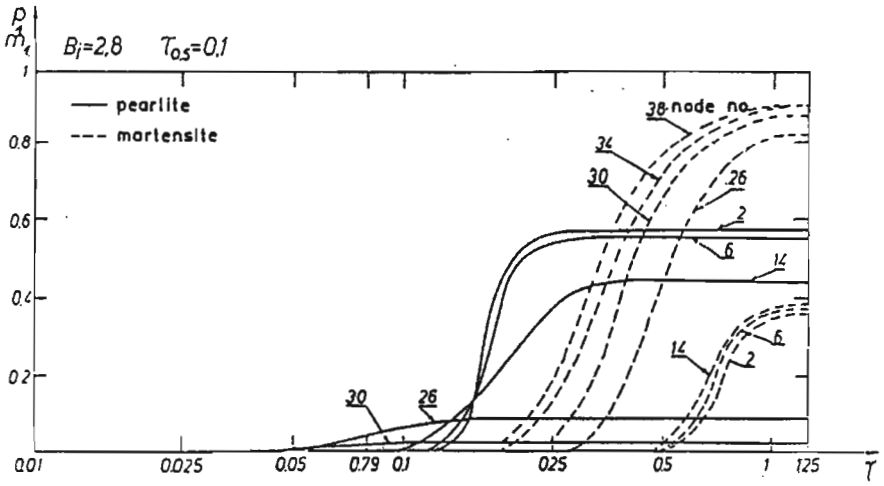

Fig. 5. Pearlite and martensite weight fraction in nodes

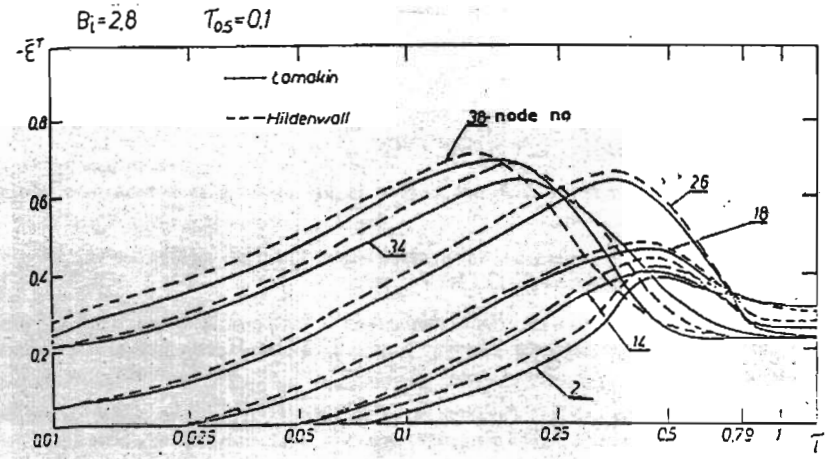

Fig. 6. Relative volumetric dilatation for spline shaft

at the nodes 2,6,14, cause that the increase of the element volume is reduced by a thermal shrinkage, because the boundary of the shaft is cold. The core is tensioned. Finally, it must be noted that the diagram of the relative change of volume presented in Fig.6 is not a working diagram. In the calculations, it is assumed that the distribution of temperatures depends only on the dimensionless Biot number Bi and for the carbon steel grades displaying the C–shaped T–T–T curves in the form of letter C. Therefore,taking into account the wide range of themperature changes during hardening (more then 1050° K), it is some kind of an approximation. For a closer estimation, the real processess could be characterized by a greater number of dimensionless parameters, but it would significantly extend the present program of numerical calculations being complicated already.

Nevertheless, the present considerably simplified calculations indicate that the method presented in this work has great potential possibilities to answer important practical questions.

Acknowledgements

The authors would like to thank Professor R.Parkitny, Technical University of Częstochowa, for rendering the FEM program available for the calculation of temperature field in 2–dimensional problems.

References

1. WOELKE J., ZIELNICA J., 1989, *Determination of transient and residual thermal-hardening stresses in steel plates*, Ingienieur – Archiv, 59, 32-42
2. LOMAKIN V.A., 1959, *Zadacha opredeleniya napruzheniĭ i deformaciĭ v processakh tekhnicheskoĭ obprabotki*, Izv. AN SSSR, OTN, 1
3. LOMAKIN V.A., 1958, *Prevrashchenie austenita pri proizvolnom rezhimie okhlazhdeniya*, Izv. AN SSSR, OTN, 2
4. LOMAKIN V.A., 1958, *Zavisimost' soprotivleniya metallov sdvigu ot ikh strukturnogo sostoyaniya*, Izv. AN SSSR, OTN, 7
5. INOUE T, RANIECKI B., 1978, *Determination of Thermal-Hardening Stress in Steels by use of Thermoplasticity Theory*, Journal of the Mechanics and Physics of Solids, 26, 3, 187-212
6. ERICSON T., HILDENWALL B., *Prediction of Residual Stresses in Case-Hardening Steels*, Department of Mechanical Engineering, S-58183, Linköping, Sweden
7. CHRISTIAN J.W., 1965, *The theory of transformation in metals and alloys*, Pergamon Press
8. CAHN I.W., *The kinetics of the pearlite reaction*, Submitted to the Journal of Metals
9. WOELKE J., 1983, *Analiza naprężeń hartowniczych w sprężystych stalowych płytach*, Rozprawy Inżynierskie, 31, 1
10. IRONS B., AHMAD S., 1980, *Techniques of Finite Elements*, Ellis Horwood

Podejście dwuwymiarowe w kinetyce przemian fazowych procesów hartowania stali

Streszczenie

W pracy przedstawiono metodykę analizy kinetyki przemian fazowych dla ciał cylindrycznych o dowolnym przekroju poprzecznym. Analizę przeprowadzono dla obszaru dwuwymiarowego, gdzie wymiana ciepła odbywa się na jego brzegu. W rozwiązaniu oparto się na metodzie wariacyjno–różnicowej, będącej połączeniem metody elementu skończonego i metody różnicowej.

Uzyskane wyniki stanowią podstawę do szacowania rozkładu pól naprężeń chwilowych i szczątkowych w procesach hartowania.

Manuscript received June 17, 1991; accepted for print April 23, 1992